Processes monitoring using adaptive confidence limit based on T-S fuzzy model and Luenberger observer

Khaled Bouzenad[1,2,3], Salah Rahmouni[1], Messaoud Ramdani[3]
[1]Laboratory of Physical Chemistry and Biology of Materials, Higher Normal School of Technological Education, Skikda, Algeria
[2]Department of Engineering, University of Quebec in Rimouski, Quebec, Canada
[3]Laboratory of Automation and Signals Annaba, Department of Electronics, Badji-Mokhtar-Annaba University, Annaba, Algeria

Article Info

Article history:

Received Feb 16, 2024
Revised Mar 24, 2024
Accepted Apr 6, 2024

Keywords:

Adaptive confidence limit
Diagnosis
Fuzzy observer
Process monitoring
T-S fuzzy model

ABSTRACT

In hazard-sensitive processes, the monitoring upsets and malfunctions correctly is an important challenge to operation safely and enhance the performance. Conventional process monitoring frequently assumes that process data follow only one Gaussian distribution, which generates a constant confidence limit and hence produces a high number of false alarms. However, in fact, industrial processes usually include various operating modes. To ovoid this drawback, the suggested approach employs an adaptive confidence limit (ACL) when a substantial number of false alarms are created. The fundamental concept underlying this study is to extract internally several local linear sub-modes of the monitored variables. In typical operating circumstances, the Gaussian mixture model (GMM) is utilized to extract several local linear sub-modes, followed by fuzzy linearization using the Takagi-Sugeno model, thereafter a bank of Luenberger observers to construct the residual spaces. An abnormal event is detected when the squared prediction error (SPE) is too great or exceeds the adaptive threshold designed to prevent the false alarms. Furthermore, an enhanced contribution plots is effectively used to identify the defective variable.

Corresponding Author:

Khaled Bouzenad
Laboratory of Physical Chemistry and Biology of Materials
Higher Normal School of Technological Education
Skikda, 21000-Algeria
Email: khaled_bzd@yahoo.fr

1. INTRODUCTION

To enhance the performance of any industrial process and correctly detect and identify any abnormal mode of the process, especially when any sensor or actuator is prone to malfunctions, the online monitoring tools become necessary [1], [2]. Numerous control technology systems have been implemented to identify and detect the faults [3]-[5]. However, the most of industrial process monitoring projects are predicated on the idea that process data follows a single Gaussian distribution (mean μ and variance σ). As a result, numerous false alerts are produced due to the confidence limit which is calculated as a constant threshold [6]-[9]. However in reality, because of process non-linearity, the process variables roughly follow a combination of Gaussian distributions (μ_j , σ_j) [10]-[14]. It should be noted that some approaches based on adaptive control limit have been proposed like [14] but the threshold remains as a straight line.

So, in this work our contribution focuses on adaptive confidence limit (ACL) leads to correctly monitor the nonlinear dynamic systems, the proposed method will be tested on sensor fault detection and identification. Gaussian mixture models (GMM) extract, under normal conditions, several operating sub-modes and allows to classify the monitored variables according to their likelihood rates of membership to the several local sub-modes, thus obtaining m local linear sub-models characterized by m Gaussian components (μ_j , σ_j), minimum message length (MML) is used during the GMM calculation to help speedly select the ideal number m of sub-modes, this technique known as fuzzy satisfactory clustering (FSC) [15], the number m is often considered known in the existing works [16]. The proposed strategy gives a multimodal behaviour using Takagi-Sugeno (T-S) fuzzy modeling allows to obtain a fuzzy linearized variables. After that, a bank of observers is used to estimate the fuzzy linearized variables and create a residual space. GMM is still being used once again for the estimated variables to extract the m sub-modes and compute their local SPE_j. The kernel density estimation (KDE) has been incorporated to acquire the local confidence limit (LCL) of each SPE_j. As result, an ACL is acquired via a weighted sum of the likelihood rates and the m local confidence limit LCL_j^{KDE} of each local SPE_j. The obtained ACL is linked to the global SPE, which gives a powerful tool capable improving the monitoring performance, reducing false alarms (nearly entirely eliminated) and detecting the commencement of process deviations earlier and more accurately than other traditional approaches.

For fault identification, to overcome the gaps of the traditional contribution plots which involves to give the contributions to the SPE(k). In a moment 'k' that can cause some errors to identify the defective sensor due to the high number of the peaks generated in the residual space. An enhanced contribution plots to the SPE is proposed which able to eliminate the unwanted peaks and correctly identify the defective sensor.

The paper is organized as follows: materials and method in section 2 introduces the monitoring tools, including the GMM for extracting m local normal sub-modes and calculating their probability rates, Takagi-Sugeno model for fuzzy linearization the monitored variables and then, bank of linear Luenberger observers to estimate the fuzzy linearized variables. The algorithm of the proposed technique is presented in this section. Section 3 is dedicated to the results and discussion, in which the effectiveness of the proposed process monitoring strategy is defended, where we discuss and assess the different obtained results. Finally, conclusions are described in section 4.

2. METHOD

The algorithm of the proposed technique involves firstly in offline a fuzzy multi-modelling during normal conditions whose aim is to obtain an ACL, usable later in online monitoring. The specified stages are explained as follows:

a. In offline under normal conditions:
   - i) The GMM tool is used at the beginning to extract the optimal number *m* of the local operation sub-modes.
   - ii) T-S fuzzy modelling to fuzzy linearize the monitored variables around the *m* operating point.
   - iii) Bank of Luenberger observers to estimate the fuzzy linearized variables.
   - iv) GMM to extract *m* fuzzy linear sub-modes of the estimated variables.
   - v) Calculation of the *m* local squared prediction error SPE_j and their local confidence limit LCL_j^{KDE}.
   - vi) The weighted sum of the probability rates ρ_j (for each local sub-mode) with m LCL_j^{KDE} (of each local SPE_j) gives the global ACL.

b. In online monitoring:
   - vii) The obtained ACL is linked to the global SPE for error detection.
   - viii) The enhanced contribution plot is used for fault identification.

2.1. Gaussian mixture model

In normal operating conditions, processes span multiple operating sub-modes so that each one is characterized by a Gaussian component. The GMM tool may be used to extract the probability density function (PDF), which is the weighted sum of the density functions of each Gaussian component. Each component is described by normal distributions with weights $\emptyset_j$, means μ_j and covariance matrix σ_j as given (1).

$$p(x|\wedge) = \sum_{j=1}^{k} \phi_j \, \mathbb{N}(x_i|y_j) \quad (1)$$

Where x∈ R^ℓ, ϕ_j is the previous probability of the jth portion and $\mathbb{N}(x_i|y_j)$ is the multivariate Gaussian density function of the jth component. The model parameters that need to be estimated for each component are ϕj and $yj = (\mu j, \sigma j)$. The updated estimated parameters ϕj, μj, and Σj are re-estimated iteratively using the expectation-maximization technique, as shown below:

– Expectation: calculate the posterior probability of the i^{th} training sample (x_i) at the k^{th} iteration:

$$p^{(k)}\left(m_j \middle| x_i\right) = \frac{\alpha_j^{(k)}\mathbb{N}\left(x_i \middle| \lambda_j^{(k)}\right)}{\sum_{l=1}^{K}\phi_l^{(k)}\mathbb{N}(x_i|\lambda_l^{(k)})} \tag{2}$$

Where m_j is the j^{th} component.

– Maximization: during the $(k + 1)^{th}$ iteration, change the model parameters:

$$\mu_j^{(k+1)} = \frac{\sum_{i=1}^{N} p^{(k)}\left(m_j \middle| x_i\right) x_i}{\sum_{i=1}^{N} p^{(k)}\left(m_j \middle| x_i\right)} \tag{3}$$

$$\alpha_j^{(k+1)} = \frac{\sum_{i=1}^{N} p^{(k)}\left(m_j \middle| x_i\right)(x_i - \mu_j^{(k+1)})(x_i - \mu_j^{(k+1)})^T}{\sum_{i=1}^{N} p^{(k)}\left(m_j \middle| x_i\right)} \tag{4}$$

$$\phi_j^{(k+1)} = \frac{\sum_{i=1}^{N} p^{(k)}\left(m_j \middle| x_i\right)}{N} \tag{5}$$

In the learning phase, parameter values are updated using the log-likelihood function as the objective:

$$\log L(x|\wedge) = \sum_{i=1}^{N} \log\left(\sum_{j=1}^{K} \phi_J \mathbb{N}\left(x_i \middle| y_j\right)\right) \tag{6}$$

where x_i is the i^{th} training sample among the total of N measurements?

In this work, the MML algorithm is used to extract the optimal number of Gaussian components [17]. Therefore, the GMM tool is used to extract m local linear sub-modes of the monitored variable and then their estimation. It should be noted that the number m of local linear sub-modes is equal to the number of Gaussian components (number of local linear sub-modes), which is equal to the number of operating points around them the linearization is done.

2.2. Fuzzy linearization by Takagi-Sugeno models

Following the extraction of the operating mode mixture, the next step is to develop fuzzy linear models [18]. The key characteristic of a T-S fuzzy model is that it expresses the local dynamics of each fuzzy implication (rule) using a linear system sub-model. The overall fuzzy model of the system is created by fuzzy mixing the linear system models [19]. The structure consisting of several sub-models with decoupled operational states, as suggested by [20], may be represented as (7).

$$\begin{cases} \dot{x}_j(t) = A_j x_j(t) + B_j u_j(t) \\ y_j(t) = C_j x_j(t) \\ y(t) = \sum_{j=1}^{m} \mu_j\left(\xi(t)\right) y_j(t) \end{cases} \tag{7}$$

Where $\dot{x}$ denotes the vector of the state variable, y denotes the vector of the output variables, m is the number of sub-models, u denotes the control variables, A_j, B_j and C_j are the matrices associated with the sub-models. Weighting function $\mu_j\left(\xi(t)\right)$ ensure the transition between the sub-modes and contribute to the overall behavior of the nonlinear system.

Where,

$$\begin{cases} \sum_{j=1}^{m} \mu_j\left(\xi(t)\right) y_j(t) = 1 \\ 0 \leq \mu_j\left(\xi(t)\right) \leq 1, \forall t > 0 \end{cases} \tag{8}$$

The global output of the multiple models is the weighted sum of the outputs of the sub-models. Each sub-model therefore has its own state space and develops there independently of the control signal and its initial state.

2.3. Bank of Luenberger observers

A Bank of observers design based on T-S fuzzy models will be utilized to estimate the fuzzy linearized variables and construct a residual space. Luenberger observers [21] are described by (9).

$$\begin{cases} \hat{x}_j(t) = \sum_{j=1}^{m} \mu_j\left(\xi(t)\right)\left(A_j x_j(t) + B_j u_j(t) + G_j e_j(t)\right) \\ \hat{y}_j(t) = C_j \hat{x}_j(t) \end{cases} \tag{9}$$

Where, G_j denotes the observed matrix gain, $\hat{x}_j(t)$ *denotes* the estimation of the state vector, $\hat{y}$ is the estimation of the output vector and $e(t) = x - \hat{x}$ is the estimation error its dynamic is given by (10).

$$\dot{e}(t) = \sum_{j=1}^{m} \mu_j(\xi(t))\,(A_j - G_j C_j e(t)) \tag{10}$$

According to Lyapunov's theorem, (10) is asymptotically stable if there is a matrix P positive and the gain matrices G_j verifying the following inequality:

$$(A_j - G_j C_j)^{\,T} P + P(A_j - G_j C_j) < 0 \tag{11}$$

linear matrix inequality (LMI) tool is used to resolve (11) [22].

2.4. Process monitoring and diagnosis

2.4.1. Squared prediction error

The difference between the observed variables and their estimates helps as an indicator for determining the occurrence and severity of abnormal events. In the literature, numerous multivariate extensions of defect detection have been proposed. The univariate statistic SPE, generated from the error e(k) following a central Chi-squared distribution, is extremely important since it represents changes in the correlation structure of the measured variables. Box [6], stated the instant 'k' is given by (12) and (13).

$$SPE(k) = e(k)\, e(k)^T \tag{12}$$

$$e(k) = x(t) - \hat{x}(t) \tag{13}$$

During the offline phase, m local SPE_j and $LCL_j^{(\mathrm{KDE})}$ must be calculated in residual subspace for different operation sub-modes. In the online phase, the global SPE(k) (which is multimodal) detects the faults in residual space. The process is deemed in an abnormal operating state at the kth observation if the global SPE(k):

$$SPE(k) > ACL^{(KDE)} \tag{14}$$

with $ACL^{(KDE)}$ denotes the adaptive control limit to be associated with the global SPE(k).

2.4.2. Adaptive control limit

After determining the constants $LCL_j^{(\mathrm{KDE})}$ of each SPE_j and the probability rates of each operation sub-mode, an adaptive control limit may be computed using the formula as (15).

$$AUCL = \sum_{j=1}^{m} \left(LCL_j^{KDE} \rho_j(k) \right), k = 1,2, \dots, n \tag{15}$$

Where during normal operation mode:
- m is the number of Gaussian components that describe local operational sub-modes.
- ρ_j is the probability rate of j^{th} sub-mode.
- The local control limit utilizing the KDE of each sub-mode is represented by$LCL_j^{(\mathrm{KDE})}$, where n is the sample count is the local control limit using the KDE of each sub-mode.
- n is the number of samples.

2.4.3. Local control limit by KDE

KDE is an effective approach for estimating PDF [23]–[27]. For a sample matrix with n variables and l samples, the density function estimator may be expressed as (16).

$$g(y, h) = \frac{1}{mh} \sum_{i=1}^{n} K\left[\frac{(x - x_i)}{h}\right] \tag{16}$$

Where h is the bandwidth statistic.

The estimator *K(.)* is the Gaussian kernel function:

$$k(x) = (2\pi)^{\frac{-n}{2}} exp\left(-\frac{1}{2} x^T x\right) \tag{17}$$

The KDE tool calculates the PDF of the SPE_j statistic. The local control limit $LCL_j^{(\mathrm{KDE})}$ may be calculated from the PDF of the SPE_j with α confidence level by solving (18).

$$\int_{\alpha}^{LCL_j^{(\mathrm{KDE})}} P(SPE_j)\, dSPE_j = \alpha, j = 1,2,\dots,m. \tag{18}$$

Where $P(SPE_j)$ denotes the PDF of the local SPE_j (under normal operating data), α is the confidence limit.

2.5. Fault identification

2.5.1. Contribution plots method

For identifying a malfunction and determine which sensor has become faulty, the most traditional technique that has been applied extensively is the contribution plots. To determine which variable has an extreme contribution to the SPE_j, this technique is often based on the contribution rate of each variable as (19).

$$cont_j^{SPE} = (e_j(k))^2 = (x_j(k) - \hat{x}_j(k))^2 \tag{19}$$

2.5.2. Enhanced contribution plots

In order to fill the gaps of the contribution graph method, which is based on the contribution rate calculated for each variable at a certain time k. When the fault sensor is detected, it may lead to errors in identifying the actual faulty variable as long as the localization is done at time k. Due to the peaks which are the residuals produced in the calculation of SPEj.

The enhanced contribution plots are applied using the average value iteratively during the sensor fault period. The $Econt_j^{SPE}$ (i) value indicates which variable has the highest average contribution to the SPEj, reflecting the present contribution. $Econt_j^{SPE}$ (i) considers all prior contributions $cont_j^{SPE}$ (i-1) using an average calculation. These average contributions are calculated before and after the moment k (and at any time gives the same result) when the indicator SPE exceeds the adaptive control limit. $Econt_j^{SPE}$ (i) can be obtained from the (20).

$$Econt_j^{SPE}\ (\mathrm{i}) = \frac{1}{\mathrm{n-k}} \sum_{\mathrm{i=k-1}}^{\mathrm{n}} cont_j^{SPE}\ (\mathrm{i}-1) \tag{20}$$

The algorithm of the enhanced contribution plots is applied for each variable, the one that gradually increases is the erroneous variable.

3. RESULTS AND DISCUSSION

This section provides an evaluation of the proposed strategy to the below bioreactor, as well as some comments on the findings acquired to assess their efficacy. It is important to note that the monitored variables must be normalized such as each variable is centered and scaled by subtracting and dividing the mean/standard-deviation from/by each column, respectively, to ensure that the results are independent of the units used. The dynamic behaviour of the bioreactor may be represented using the following nonlinear model:

$$\begin{cases} \dot{S}(t) = D(t)\big(S_{in}(t) - S(t)\big) - k\, r(t) \\ \quad\dot{X}(t) = -D(t)X(t) + r(t) \end{cases} \tag{21}$$

Where,
- *S(t)* and *X(t)* are the concentration rates of the carbon substrate and that of the biomass.
- $D(t) > 0$ is the dilution rate (A varied square wave signal with noise influence).
- *k* is an efficiency coefficient.
- S_{in} is the substrate feed concentration rate.
- *r(t)* is the speed production of the biomass described by the following expression:

$$r(t) = \frac{\mu_{max} S(t) X(t)}{K_s + S(t)} \tag{22}$$

Where,
- The maximal specific growth rate and the saturation constant are denoted by μ_{max} and K_s , respectively.
- In this simulation test $\mu_{max} = 0.33h^{-1}$, $K_s = 5\ l^{-1}$, $k = 20$ and $S_{in}(t)$ is square shaped with variable amplitude.

3.1. Multi-modelling of the monitored variables

Under normal operating conditions, Figure 1 show the multi-modeling of the monitored variables, where the fuzzy linearized variables (Smm(t), Xmm(t)) and the real variables (SBio(t), XBio(t)) are plotted in Figure 1(a). The number of local linear sub-modes m=3 corresponds to the number of activation functions $\mu_j(\xi(t))$ in Figure 1(b), which reflect the weights belonging of the sub-models in the global model. Figure 2 illustrates the fuzzy linearized variables (Smm(t), Xmm(t)) and their estimates (Sobs(t), Xobs(t)) using banks of Luenberger observers with m=3 local linear observers. It is apparent that the measured variables (SBio(t), XBio(t)) of the bioreactor have been correctly approximated.

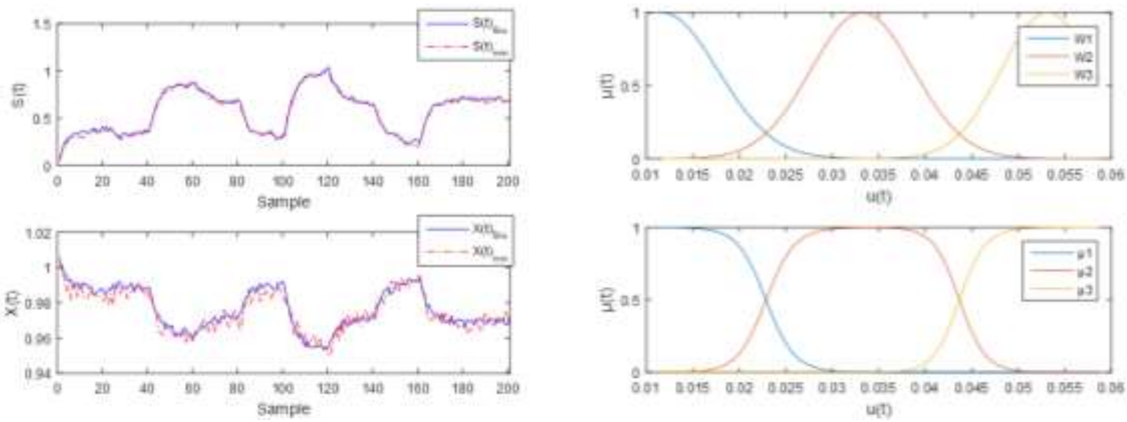

(a) (b)

Figure 1. Multi-modelling of the monitored variables (a) estimated variables using T-S fuzzy model and (b) activation functions $\mu_j(\xi(t))$

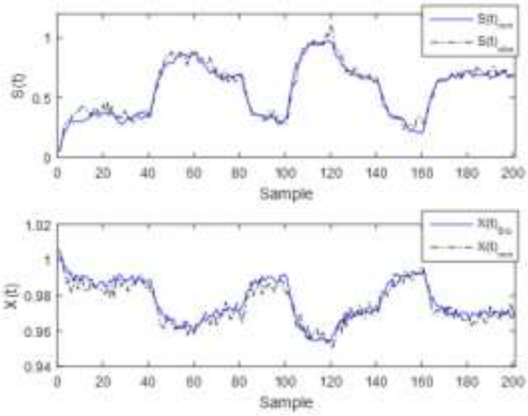

Figure 2. Estimated variables using Luenberger observers

3.2. Process monitoring

Figures 3 depict the filtered SPE linked to the ACL (confidence level 95%) where the Figure 3(a) shows the monitoring during normal operating conditions (no faults). To more reduce the false alarms, an exponentially weighted moving average (EWMA) is employed to filter the influence of outliers and noise. The filter is applied to the SPE inserts an important quality and completely eliminate the false alerts. As was mentioned in section 1 the proposed adaptive control limit like in [14] the threshold remains as a straight line, whilst our proposed strategy is based on the ACL not a straight line which gives a powerful contribution to the processes monitoring field. In the abnormal case, as shown in Figure 3(b), it can be observed, the SPE indicator surpasses its ACL at the time k=130 (the moment when the fault was inserted).

The result shows the robust performance of the proposed strategy in the absence or presence of faults which produces few alarms (almost zero), fast, early, and safe in detection. Compared to conventional methods it is clear that when using ACL, the fault is easily, correctly, and quickly detected, because if there was an upper control limit (straight line) and its value was considerable to avoid false alarms and the fault was drift type, the detection will be slow and delayed compared to our proposed ACL.

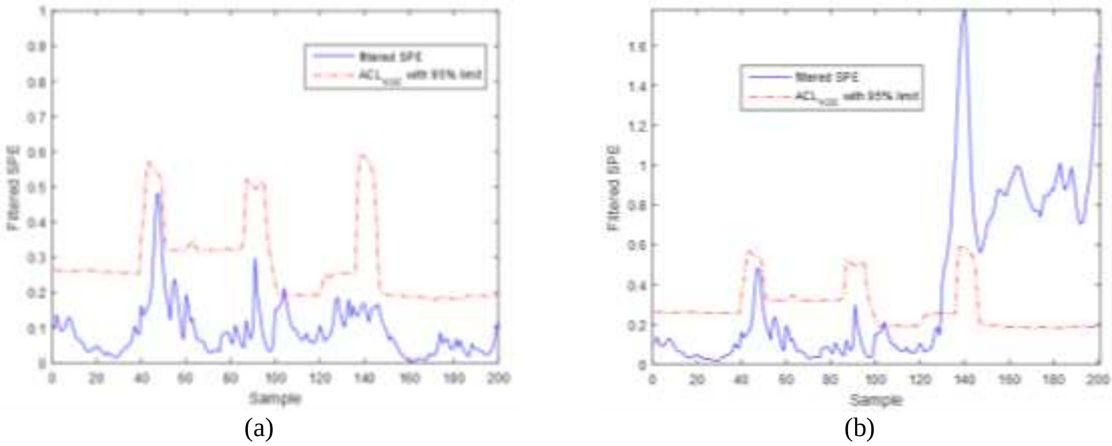

Figure 3. Filtered SPE with ACL (a) during normal state and (b) under drift fault

In the previous figure (Figure 3(b)), nothing can be concluded for identification, enhanced contribution plots technique is employed in below for completing the monitoring operation and discovering the defective variable.

3.3. Fault identification

Once a malfunction has been found, it is required to locate the defective sensor. According to the enhanced contribution plots version, as shown in Figure 4, the sensor's highest contribution to the SPE is the defective sensor. The disadvantages of classical contribution plots were solved using an upgraded of contribution plots, as seen in the in Figure 4. $Econt_J^{SPE}$ (i) can be accurately and quickly presented online as soon as any malfunction is discovered. The Figure 4 depicts the filtered SPE, which does not include any undesired peaks that might cause identification problems.

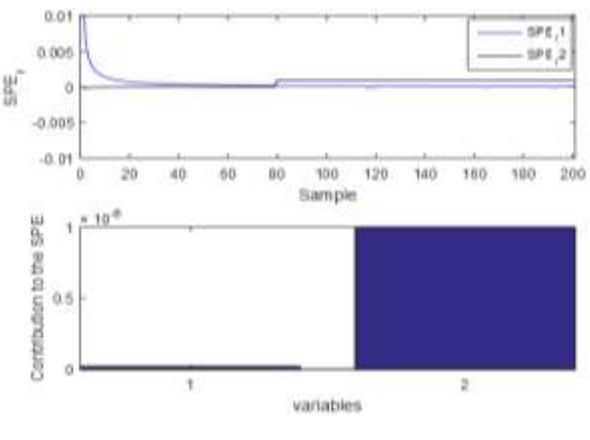

Figure 4. Fault identification using enhanced contribution plots

This study investigated the effects of unwanted peaks that cause false alarms in the monitoring and therefore may possibly cause identification problems, while earlier studies have explored the impact of false alarms. They could not eliminate it completely and they have not explicitly addressed its influence on the identification phase. We found that false alarms correlate with the unwanted peaks which come clearly from the residual space. The proposed method in this study tended to have a higher proportion of avoiding inordinately the unwanted peaks by an adaptive control limit. Our study suggests that higher unwanted peaks are not associated with the poor performance of FSC, the proposed method may benefit from increasing the number of linear local models without adversely impacting the algorithm. This study explored a comprehensive model-based monitoring. However, further and in-depth studies may be needed to confirm its performance on systems that have a high number of variables, especially regarding monitoring without behavioural models. Our study demonstrates that the model-based monitoring using adaptive control limits is more resilient than those that use a traditional threshold in which its value is made constant. Future studies may explore diagnosis under periodic non-steady conditions, with feasible ways of producing a useful adaptive control.

4. CONCLUSION

Our findings give clear proof that the phenomena of unwanted peaks can pose significant difficulty in accurately detecting and recognizing any aberrant operating mode. The provided observations suggest that our method has superior performance and is more efficient for processes monitoring and fault diagnosis, because traditional methods are sensitive to false alarms due to their constant threshold (a straight line), and the upper confidence limit is considered slow for fault detection because their upper value of the threshold, which is typically considered too large to avoid false alarms. Furthermore, the typical contribution plot approach for fault diagnosis is unreliable due to undesired peaks. So, as compared to traditional approaches, the ACL can reduce an excessive number of false alarms, and the abnormal event is identified as promptly and reliably as possible if the squared prediction error exceeds the adaptive threshold. Furthermore, an upgraded contribution plot approach is used to accurately identify the observed problematic variable, resulting in a higher diagnostic rate.

REFERENCES

[1] E. Juuso and D. Galar, Eds., *Proceedings of the 5th International Conference on Maintenance, Condition Monitoring and Diagnostics 2021*. Singapore: Springer Nature Singapore, 2023.

[2] M. Kano and Y. Nakagawa, "Data-based process monitoring, process control, and quality improvement: recent developments and applications in steel industry," *Computers & Chemical Engineering*, vol. 32, no. 1–2, pp. 12–24, Jan. 2008, doi: 10.1016/j.compchemeng.2007.07.005.

[3] K. Malinowski, T. J. McAvoy, R. George, S. Dieterich, and W. D. D'Souza, "Online monitoring and error detection of real-time tumor displacement prediction accuracy using control limits on respiratory surrogate statistics," *Medical Physics*, vol. 39, no. 4, pp. 2042–2048, Apr. 2012, doi: 10.1118/1.3676690.

[4] S. Abdelmalek, L. Barazane, A. Larabi, and M. Bettayeb, "A novel scheme for current sensor faults diagnosis in the stator of a DFIG described by a T-S fuzzy model," *Measurement*, vol. 91, pp. 680–691, Sep. 2016, doi: 10.1016/j.measurement.2016.05.102.

[5] W. Bougheloum, M. Bekaik, and S. Gherbi, "Multimode system condition monitoring using sparsity reconstruction for quality control," *International Journal of Electrical and Computer Engineering (IJECE)*, vol. 13, no. 3, pp. 2711–2720, Jun. 2023, doi: 10.11591/ijece.v13i3.pp2711-2720.

[6] G. E. P. Box, "Some Theorems on quadratic forms applied in the study of analysis of variance problems, I. effect of inequality of variance in the one-way classification," *The Annals of Mathematical Statistics*, vol. 25, no. 2, pp. 290–302, Jun. 1954, doi: 10.1214/aoms/1177728786.

[7] K. Bouzenad, M. Ramdani, N. Zermi, and K. Mendaci, "Use of NLPCA for sensors fault detection and localization applied at WTP," in *2013 World Congress on Computer and Information Technology (WCCIT)*, Jun. 2013, pp. 1–6, doi: 10.1109/WCCIT.2013.6618761.

[8] K. Bouzenad, M. Ramdani, and A. Chaouch, "Sensor fault detection, localization and reconstruction applied at WWTP," in *2013 Conference on Control and Fault-Tolerant Systems (SysTol)*, Oct. 2013, pp. 281–287, doi: 10.1109/SysTol.2013.6693917.

[9] A. Chaouch, K. Bouzenad, and M. Ramdani, "Enhanced multivariate process monitoring for biological wastewater treatment plants," *International Journal of Electrical Energy*, pp. 131–137, 2014, doi: 10.12720/ijoee.2.2.131-137.

[10] K. Bouzenad and M. Ramdani, "Multivariate statistical process control using enhanced bottleneck neural network," *Algorithms*, vol. 10, no. 2, 2017, doi: 10.3390/a10020049.

[11] F. E. Laumal, H. Suhardiyanto, M. Solahudin, and S. Widodo, "Optimal sensor location for adaptive control system in tropical smart greenhouse," *Indonesian Journal of Electrical Engineering and Computer Science*, vol. 30, no. 3, pp. 1449–1457, Jun. 2023, doi: 10.11591/ijeecs.v30.i3.pp1449-1457.

[12] U. Anand Trilokinath and S. Kumar Singh, "Analysis of BBNs over fault detection and diagnosis in industrial application," *Indonesian Journal of Electrical Engineering and Computer Science*, vol. 9, no. 1, pp. 68–72, Jan. 2018, doi: 10.11591/ijeecs.v9.i1.pp68-72.

[13] G. P. N. Hakim, R. Muwardi, M. Yunita, and D. Septiyana, "Fuzzy Mamdani performance water chiller control optimization using fuzzy adaptive neuro fuzzy inference system assisted," *Indonesian Journal of Electrical Engineering and Computer Science*, vol. 28, no. 3, pp. 1388–1395, Dec. 2022, doi: 10.11591/ijeecs.v28.i3.pp1388-1395.

[14] T. Wang *et al.*, "An adaptive confidence limit for periodic non-steady conditions fault detection," *Mechanical Systems and Signal Processing*, vol. 72–73, pp. 328–345, May 2016, doi: 10.1016/j.ymssp.2015.10.015.

[15] N. Li, S.-Y. Li, and Y.-G. Xi, "Multi-model predictive control based on the Takagi–Sugeno fuzzy models: a case study," *Information Sciences*, vol. 165, no. 3–4, pp. 247–263, Oct. 2004, doi: 10.1016/j.ins.2003.10.011.

[16] K. Ouarid, M. Essabre, A. El Assoudi, and E. H. El Yaagoubi, "State and fault estimation based on fuzzy observer for a class of Takagi-Sugeno singular models," *Indonesian Journal of Electrical Engineering and Computer Science*, vol. 25, no. 1, pp. 172–182, Jan. 2022, doi: 10.11591/ijeecs.v25.i1.pp172-182.

[17] M. A. T. Figueiredo and A. K. Jain, "Unsupervised learning of finite mixture models," *IEEE Transactions on Pattern Analysis and Machine Intelligence*, vol. 24, no. 3, pp. 381–396, Mar. 2002, doi: 10.1109/34.990138.

[18] A. M. Nagy-Kiss and G. Schutz, "Estimation and diagnosis using multi-models with application to a wastewater treatment plant," *Journal of Process Control*, vol. 23, no. 10, pp. 1528–1544, Nov. 2013, doi: 10.1016/j.jprocont.2013.09.027.

[19] T. Takagi and M. Sugeno, "Fuzzy identification of systems and its applications to modeling and control," *IEEE Transactions on Systems, Man, and Cybernetics*, vol. SMC-15, no. 1, pp. 116–132, Jan. 1985, doi: 10.1109/TSMC.1985.6313399.
[20] D. Filev, "Fuzzy modeling of complex systems," *International Journal of Approximate Reasoning*, vol. 5, no. 3, pp. 281–290, May 1991, doi: 10.1016/0888-613X(91)90013-C.
[21] M. Zeitz, "The extended Luenberger observer for nonlinear systems," *Systems & Control Letters*, vol. 9, no. 2, pp. 149–156, Aug. 1987, doi: 10.1016/0167-6911(87)90021-1.
[22] S. Boyd, L. El Ghaoui, E. Feron, and V. Balakrishnan, *Linear matrix inequalities in system and control theory*. SIAM, 1994.
[23] T. Chen, J. Morris, and E. Martin, "Probability density estimation via an infinite gaussian mixture model: application to statistical process monitoring," *Journal of the Royal Statistical Society Series C: Applied Statistics*, vol. 55, no. 5, pp. 699–715, Nov. 2006, doi: 10.1111/j.1467-9876.2006.00560.x.
[24] S. Lee and J. Chai, "An enhanced prediction model for the on-line monitoring of the sensors using the Gaussian process regression," *Journal of Mechanical Science and Technology*, vol. 33, no. 5, pp. 2249–2257, May 2019, doi: 10.1007/s12206-019-0426-7.
[25] P.-E. P. Odiowei and Yi Cao, "Nonlinear dynamic process monitoring using canonical variate analysis and Kernel density estimations," *IEEE Transactions on Industrial Informatics*, vol. 6, no. 1, pp. 36–45, Feb. 2010, doi: 10.1109/TII.2009.2032654.
[26] J. Liang, "Multivariate statistical process monitoring using kernel density estimation," *Developments in Chemical Engineering and Mineral Processing*, vol. 13, no. 1–2, pp. 185–192, Jan. 2005, doi: 10.1002/apj.5500130117.
[27] W. Fan, S. Ren, C. Yu, H. Yu, P. Wang, and F. Si, "A mixture of probabilistic predictable feature analysis for multi-mode dynamic process monitoring," *Journal of the Taiwan Institute of Chemical Engineers*, vol. 143, p. 104635, Feb. 2023, doi: 10.1016/j.jtice.2022.104635.

BIOGRAPHIES OF AUTHORS

Khaled Bouzenad is an Associate Professor at the Higher Normal School of Technical Education (ENSET), Skikda, Algeria. He Holds a Ph.D. degree in Automatic Control from The University Badji Mokhtar of Annaba. His research areas are statistical process monitoring, machine learning, environmental and biosystems engineering and fuzzy systems. He can be contacted at email: khaled_bzd@yahoo.fr.

Salah Rahmouni Ph.D. degree in engineering, professor, head of Department and Head of a research team in a research laboratory at the Higher Normal School of Technological Education (ENSET), SKIKDA, Algeria. Her research interests include photovoltaics, magnetic field, solar energy, porous silicon, electrochemical anodization. He can be contacted at email: rahmouni.eln@gmail.com.

Messaoud Ramdani received his doctorat d'Etat (Ph.D. degree) in Automatic Control from the University of Annaba, Algeria, in 2006. From 2003 to 2005, he has held student research visiting position at the Research Centre for Automatic Control of Nancy (CRAN), University of Lorraine, Nancy, France. He is currently a Professor at the Department of Electronics, Faculty of Engineering, University Badji Mokhtar-Annaba, Algeria. His current research interests include fuzzy systems, machine learning, model predictive control, environmental and biosystems engineering, smart farming systems, statistical process monitoring, intelligent data analysis and the application of computational intelligence. He is responsible for several research projects. Member of International Journal of Automation and Control (IJAAC)". "International Journal of Cybernetics and Cyber-Physical Systems" and referee on several reputable conferences and journals. He can be contacted at email: mes_ramdani@yahoo.com.